Received: 19 March 2021 | Revised: 21 April 2021 | Accepted: 21 April 2021

DOI: 10.1002/pol.20210192

RESEARCH ARTICLE

JOURNAL OF POLYMER SCIENCE WILEY

Cyclic allylic sulfide based photopolymer for holographic recording showing high refractive index modulation

Paola Galli[1] | **Richard A. Evans**[2] | **Chiara Bertarelli**[3] | **Andrea Bianco**[1]

[1]INAF—Osservatorio Astronomico di Brera, Merate, Italy

[2]CSIRO Manufacturing, Research Way, Clayton, Victoria, Australia

[3]Politecnico di Milano, Dipartimento di Chimica, Materiali e Ingegneria Chimica, P.zza Leonardo da Vinci 32, Milan, Italy

Correspondence
Paola Galli and Andrea Bianco, INAF—Osservatorio Astronomico di Brera, via Bianchi 46, 23807 Merate, Italy.
Email: paola.galli@inaf.it (P. G.) and andrea.bianco@inaf.it (A. B.)

Funding information
Fondazione Cariplo (IT); OPTICON H2020, Grant/Award Number: 730890; Materiali Avanzati; Regione Lombardia

Abstract

The development and characterization of a new holographic photopolymer system showing high refractive index modulation (Δn) is presented. It exploits the ring-opening polymerization reaction of a cyclic allylic sulfide (CAS) monomer, which is dispersed in a cellulose acetate butyrate (CAB) polymer matrix together with a blue sensitive radical photoinitiator. Volume Phase Holographic Gratings (VPHGs) obtained using these films show a very good fidelity of the transferred pattern, without deviations from the theoretical curves. A high Δn is obtained due to the addition to this system of a tetrafunctional thiol crosslinker, which maximizes the material potential (formula limit) of the formulation. It also allows for a thermal post process of the gratings, further enhancing the Δn. The photopolymer properties are evaluated as function of the monomer and thiol concentration to determine the optimal composition, at which a Δn greater than 0.03 is obtained. This is a considerably high value in the field of photopolymers for holography and it enables the manufacturing of efficient holograms.

KEYWORDS

cyclic allylic sulfides, holography, photopolymers, refractive index modulation, thiol-ene polymerization

1 | INTRODUCTION

Photopolymers are being largely studied for holographic applications and in particular for volume phase holograms (lenses, data storage)[1–4] and devices (waveguides)[5,6] thanks to their appealing and unique properties[7–9]: their formulation is highly versatile, they can be deposited by means of different techniques in a wide range of thickness, the transfer of the holographic pattern is easy and the material does not require any cumbersome wet developing post-process (i.e. they are self-developing). Such nice features, pushed Covestro to develop commercial high performance Bayfol® HX photopolymers for holography.[10–12] However, the modulation of the refractive index (Δn) reachable by photopolymer is still limited if compared to dichromated gelatins[13,14] or silver halides,[15] which are the reference holographic materials in terms of this property. This prevents the use of photopolymers in some fields, such as dispersing elements for high-performances spectrographs or high efficiency and thin lenses.

The mechanism for hologram formation in photopolymers is based on photoinduced polymerization and mass transfer of monomers dispersed in a binder. When

This is an open access article under the terms of the Creative Commons Attribution-NonCommercial-NoDerivs License, which permits use and distribution in any medium, provided the original work is properly cited, the use is non-commercial and no modifications or adaptations are made.
© 2021 The Authors. *Journal of Polymer Science* published by Wiley Periodicals LLC.

the material is illuminated with an interference pattern, photoinitiators are activated only in the areas of constructive interference, where monomers are therefore consumed. This leads to the formation of a concentration gradient that causes the migration of monomers from dark to bright areas, where the polymer chains growth.[6,7,16,17] Consequently, the refractive index modulation in photopolymers originates from two main factors: (i) a density increase and (ii) a separation of index contrasting species (monomer and binder). The density increase is due to both mass transport and polymerization reaction and it may also be a source of unwanted distortions in the exposed material.[18–20] A parallel approach is at the basis of photopolymerizable nanoparticle-polymer composite (NPC), where there is a mutual diffusion of the reactive monomer from the dark to the bright areas and the inert nanoparticles from the bright to the dark areas.[21–23] Exploiting the mismatch of the refractive index and using hyperbranched-polymer (HBP) organic nanoparticles, Tomita et al have been able to reach Δn of the order of 0.03 and 0.045 depending on the composition and writing wavelength.[24,25] Considering the standard photopolymers, only a certain fraction of the monomer present in the formulation usually diffuses and polymerizes with the desired spatial distribution, thus contributing to Δn.[26,27] This limitation in the Δn may be mitigated by increasing the concentration of the active monomer, but a solubility limit exists and it depends on the monomer/matrix combination.[28] Moreover, it is not effective to have unreacted species inside the film that have to be consumed during the bleaching step (i.e. homogeneous post-exposure made to consume unreacted species after the holographic writing). Therefore, it is apparent that increasing the monomer migration and conversion is highly desirable. A strategy to achieve a higher monomer conversion can be the addition of thiols to the photopolymer formulation to promote the thiol-ene reaction. Thiol-enes polymerize by a step-growth radical mechanism[29] with the onset of gel formation for crosslinked networks delayed compared to acrylates.[30] This allows for reaching a higher conversion of functional groups. A similar approach has been used by McLeod et al, showing interesting results in terms of dynamic range (up to 0.04).[31]

Herein, we developed a new photopolymer formulation based on the combination of a cyclic allylic sulfide (CAS) monomer, 7-methylene-1,5-dithiacyclooctan-3-yl acetate (MDTOA), and a tetrafunctional thiol. A very high refractive index modulation is achieved and, by the addition of the thiol, it can be increased from 35% to 86% of the formula limit, that is the maximum refractive index modulation that can be theoretically achieved in case of ideal separation of index contrasting species.

CAS monomers undergo a free-radical ring-opening polymerization reaction, that contrary to common free-radical polymerizations, does not suffer from large polymerization-induced shrinkage.[32–34] Moreover, there is no problem of film stability that is typical of cationic or anionic ring-opening monomer.[7,35] Indeed, ionic polymerizations require acid initiators with consequent release of acid species that could degrade the polymeric film. This problem is avoided with CAS monomers, which polymerize via a radical mechanism. Although this kind of reaction has been little exploited so far, it has led to promising results.[36] The use of the selected CAS monomer together with a tetrafunctional thiol as crosslinker allows for the exploitation of almost all the potential dynamic range of the mixture. The new photopolymer formulation was tested through the writing of transmission Volume Phase Holographic Gratings (VPHGs). They are the simplest volume phase holograms where a periodic modulation of the refractive index is impressed in the volume of a film of constant thickness. They are commonly used as dispersing elements for spectroscopy. After the writing of the hologram, the samples are thermally treated to restore mobility to the system and to promote local density variations in the grating.[37,38] This process leads to a remarkable increase of the Δn when a fully crosslinked network is formed.

2 | RESULTS AND DISCUSSION

In this section, the results are reported starting from the description of the photopolymer formulation, followed by the holographic writing and characterization before and after the thermal treatment.

2.1 | Photopolymer formulation

The photopolymer formulation consists in a high molecular weight binder in which the writing chemistry is dissolved. Cellulose acetate butyrate (CAB) is chosen thanks to its high transparency and good filmability; moreover, it has been already used in photopolymer systems.[37,39] The selected writing monomer is 7-methylene-1,5-dithiacy clooctan-3-yl acetate (MDTOA); its chemical structure is shown in Figure 1.

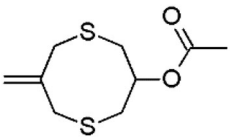

FIGURE 1 Chemical structure of the cyclic allylic sulfide monomer 7-methylene-1,5-dithiacyclooctan-3-yl acetate (MDTOA)

The concentration of MDTOA was varied from 4 to 24 wt%. A plasticizer, Citrofol AHII, was used in the formulation to favor monomer migration during the holographic exposure.[37] The tetrafunctional thiol (pentaery thritol tetrakis[3-mercaptopropionate], PETMP) was added to some samples in molar ratios of thiol groups to MDTOA of 0.25:1, 0.5:1 or 1:1; it acts as crosslinker and it is used to promote the thiol-ene polymerization.[30,40] Bis (2,6-difluoro-3-[1-hydropyrrol-1-yl]phenyl)titanocene (also known as Irgacure® 784, I784) is a cleavage type photoinitiator, which forms radicals upon light exposure[41,42]; its concentration was adjusted in order to have a film absorbance of about one at the writing wavelength (457 nm); the absorption curve of a film before and after bleaching is reported in Figure 2. Having a high film absorbance in correspondence of the wavelength used for holographic recording was demonstrated to be crucial for the formation of a stable pattern, as discussed in a previous work.[43]

The polymerization mechanism of MDTOA is reported in Scheme 1, and consists in the radical addition to the C═C bond of the monomer to give the scission of the carbon-sulfur bond followed by the formation of a new C═C bond and a thiyl radical, which can propagate and further react.[44] Although all reaction steps are reversible, the relief of ring strain by ring-opening of the intermediate radical drives the reaction forward the polymer formation.

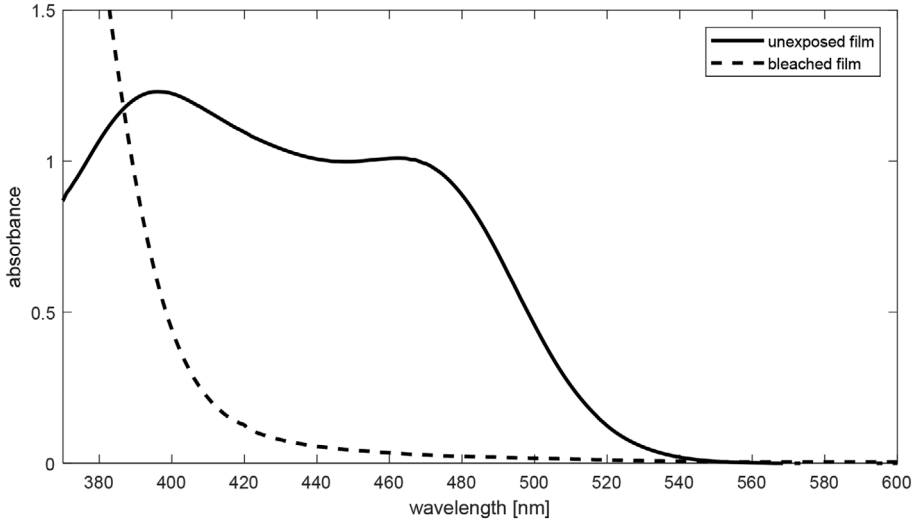

FIGURE 2 UV–vis absorption spectra of a 18 μm-thick photopolymer film before and after bleaching

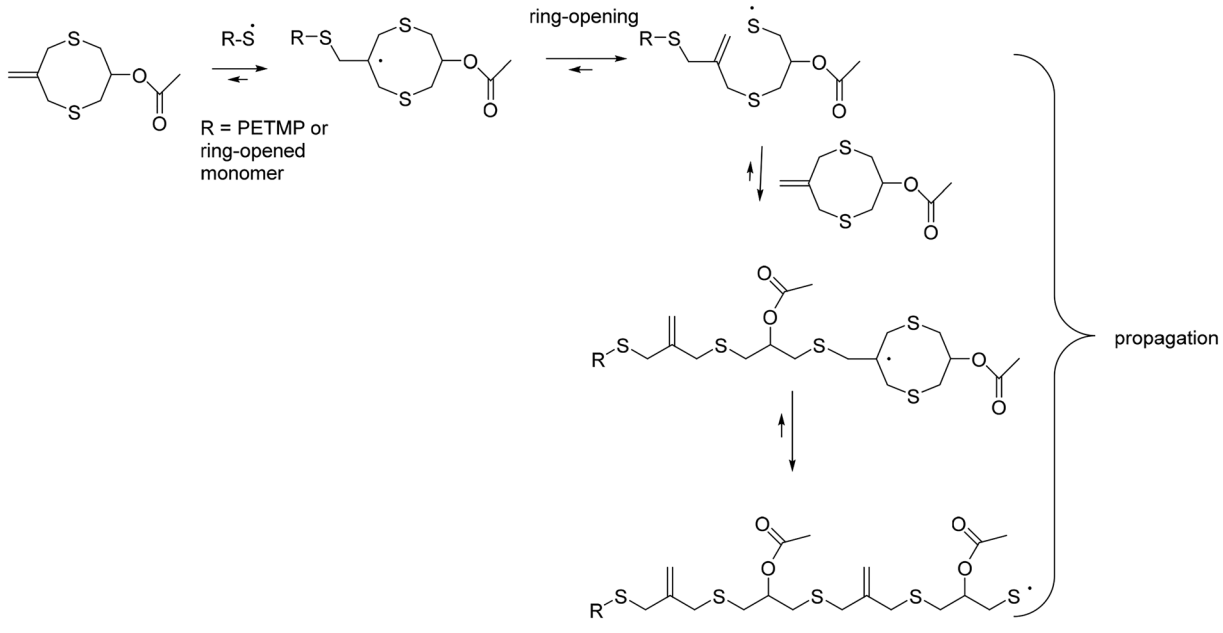

SCHEME 1 Polymerization mechanism of MDTOA monomer

The addition of thiols to the photopolymer formulation promotes a thiol-ene addition. Therefore, the radicals formed by the cleavage of I784 can also cause the lysis of S—H bond of PETMP, followed by the addition of the thiyl radical to the carbon of ene functionality of the monomer. Moreover, the PETMP thiyl radical can also add to the polymer backbone forming an intermediate radical, as illustrated in Scheme 2. The intermediate

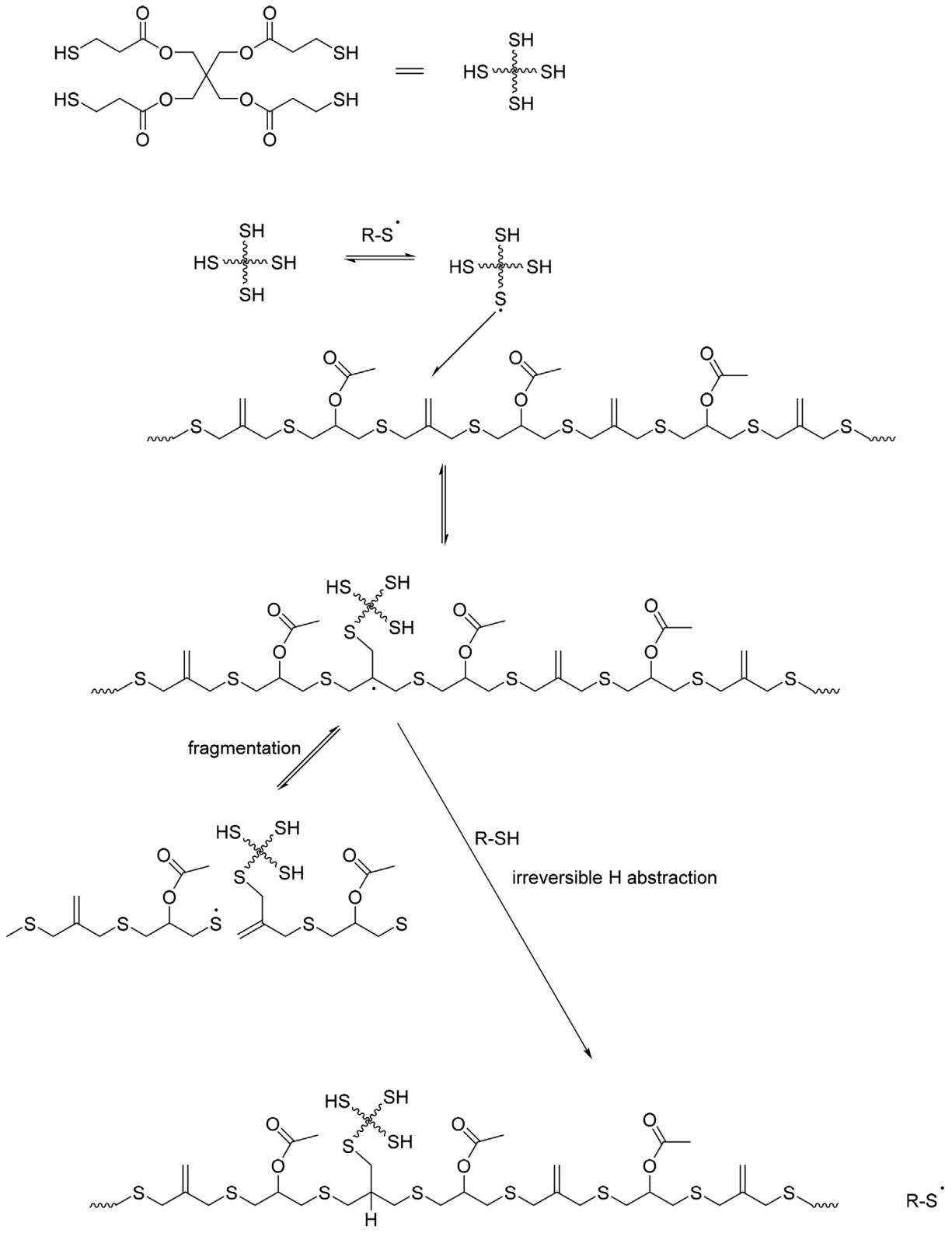

SCHEME 2 Crosslinking mechanism by PETMP addition to polymer backbone

TABLE 1 Composition of the photopolymers under investigation for 1.4 ml of solvent with corresponding measured n_{ave} values and computed Δn_{limit}

Photopolymer formulation	Sample	Component (mass, mg)					Refractive index	
		MDTOA	PETMP	CAB	Plasticizer	I784	n_{ave}	Δn_{limit}
MDTOA/I784	1[a]	84	—	250	100	100	1.5214	0.0172
MDTOA/PETMP/I784 (variable PETMP concentration)	2	84	11.8	250	100	100	1.5218	0.0176
	3	84	23.6	250	100	100	1.5221	0.0179
	4[a]	84	47.2	250	100	100	1.5225	0.0183
MDTOA/PETMP/I784 (variable MDTOA concentration and MDTOA/thiol 1:1)	5[a]	21	11.8	250	100	100	1.5182	0.0140
	6[a]	42	23.6	250	100	100	1.5205	0.0163
	7[a]	63	35.2	250	100	100	1.5215	0.0173
	4[a]	84	47.2	250	100	100	1.5225	0.0183
	8[a]	126	70.8	250	100	100	1.5271	0.0229
	9[a]	168	94.4	250	100	100	1.5283	0.0241
PETMP/I784	10	—	47.2	250	100	100	1.5144	0.0102

[a]Samples thermally treated at 120°C for 2.5 h after the holographic writing.

radical can fragment with consequent expulsion of the thiyl radical that just added or it can cleave the polymer backbone. However, the intermediate radical can also abstract a hydrogen atom irreversibly to give thiol-ene addition to the polymer backbone promoting a crosslinking. When a significant amount of thiol is present in the photopolymer formulation (e.g. MDTOA: thiol = 1:1), the irreversible thiol-ene reaction is favored over polymer fragmentation.

In order to predict the performances in terms of refractive index modulation (Δn) of a photopolymer system, the formula limit (Δn_{limit})[27] can be computed. It corresponds to the difference between the refractive index of the mixture (n_{ave}) and the refractive index of the background material (n_1): $\Delta n_{limit} = n_{ave} - n_1$. In this case, the background material is intended the mixture of CAB, plasticizer and I784. The refractive indices n_{ave} and n_1 were determined experimentally by Abbe measurements, as described in the experimental section. The n_{ave} values are reported in Table 1 together with the computed Δn_{limit} for the different photopolymer compositions. The measured refractive index for the background material (n_1) is 1.5042.

The refractive index of the mixture increases at increasing monomer concentration, as expected, MDTOA being the high-index component of the formulation ($n_{\mathrm{MDTOA}} = 1.5613$). Also PETMP ($n_{\mathrm{PETMP}} = 1.531$) contributes at increasing n_{ave}, which is higher for the MDTOA/PETMP/I784 formulation than for MDTOA/I784 formulation at same monomer concentration.

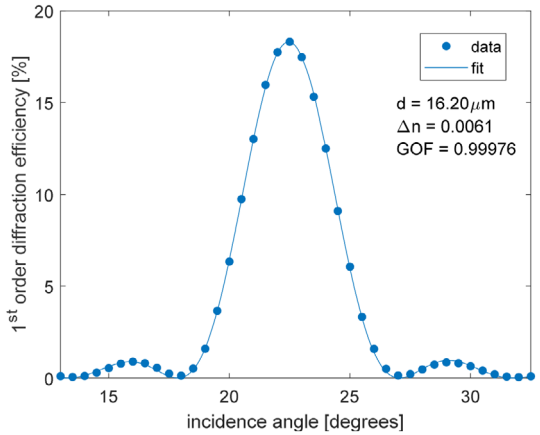

FIGURE 3 Diffraction efficiency curve of sample 1 measured at 632.8 nm (p- polarization) as function of the incidence angle with relative fit with the Kogelnik equation

2.2 | VPHG writing

For the writing of the VPHG, a dose of 0.48 J/cm^2 was used for the MDTOA/I784 photopolymer formulation. The diffraction efficiency curve measured at 632.8 nm with the relative fit for sample 1 is reported in Figure 3.

The film has a thickness of 16.2 μm and a line density of 1213 lines/mm. The Kogelnik equation fits the experimental curve with high fidelity, meaning that the sinusoidal light profile is well transferred in the material as a sinusoidal refractive index modulation. The Δn achieved

is of 0.0061, which corresponds to 35% of the formula limit. This result is consistent with the studies reported in the literature,[27,37] where it is shown that the usable fraction of Δn_{limit} is between 30% and 60% for photopolymer formulations using CAB as binder. The diffraction efficiency was remeasured after 1 month without any apparent change, proving that the grating is stable in time, as also reported in a previous work.[43]

A further analysis of the photopolymer reaction was performed by means of IR spectroscopy. Firstly, the IR spectrum of MDTOA and the corresponding polymer obtained by photopolymerization (irradiation at 254 nm, total dose of 4 J/cm^2) were recorded and are reported in Figure 4.

As we can see, the spectrum of the monomer and the one of the polymer show many similar signals since the same chemical groups are present. For example the C═O stretching is found at about 1740 cm^{-1} and the —CH$_3$ umbrella at 1379 cm^{-1} in both cases. The peak related to the C═C stretching (1632 cm^{-1}), whose disappearance is usually monitored to analyze the monomer consumption during the polymerization reaction, in this particular case is still present in the polymer at 1636 cm^{-1}. The small shift in the vibration frequency of this peak is due to the different position of the group before and after polymerization. Similarly, the peak related to the C—O asymmetric stretching is found at 1236 cm^{-1} for the monomer and at 1232 cm^{-1} for the polymer. Moreover, there is a difference in the shape and width of this peak, meaning that, in the case of the polymer, more normal modes contribute to this band. As for the C—O symmetric stretching, the band is shifted from 1022 to 1026 cm^{-1} passing from the monomer to the polymer. A significant change is observed for the monomer bands at 991 and 960 cm^{-1}, related to the vinyl ═CH$_2$ twisting and C—C stretching,[45,46] which are very weak in the polymer spectrum probably due to a completely different coupling of these vibrational modes after the opening of the ring. The variation of some characteristic bands was found also in the spectra of the photopolymer mixture (Figure 5). Since the signals of the matrix are very intense, the spectrum of a film containing only CAB and plasticizer was recorded and subtracted from the spectra of the grating and of the unexposed photopolymer.

The comparison of the two spectra gives a qualitative indication of photoinitiator consumption and of monomer reaction. In particular, we clearly notice the

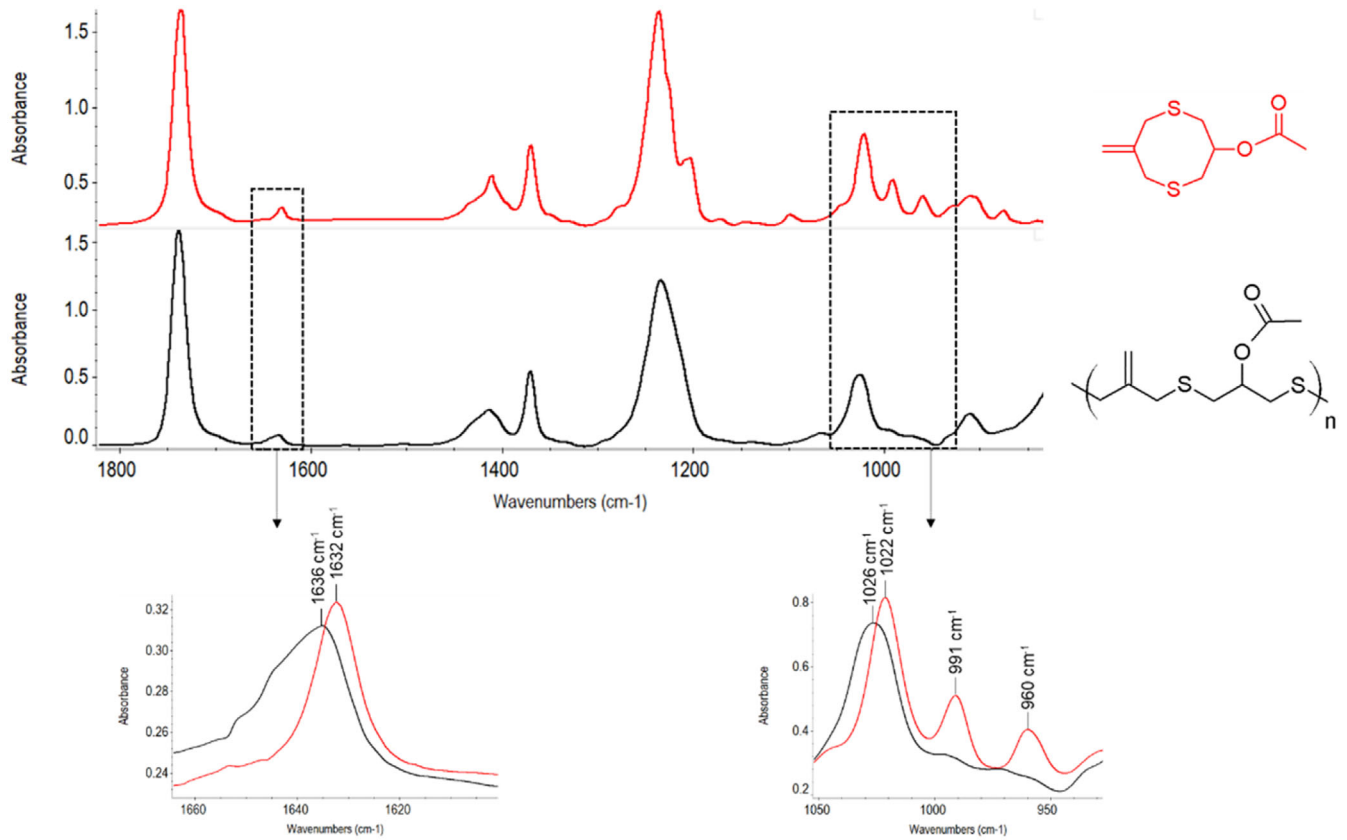

FIGURE 4 IR spectrum of monomer MDTOA (red line) and the resulting polymer obtained by photopolymerization (black line) with magnification of the C═C stretching region (1660–1610 cm^{-1}) and of the 1050–930 cm^{-1} region

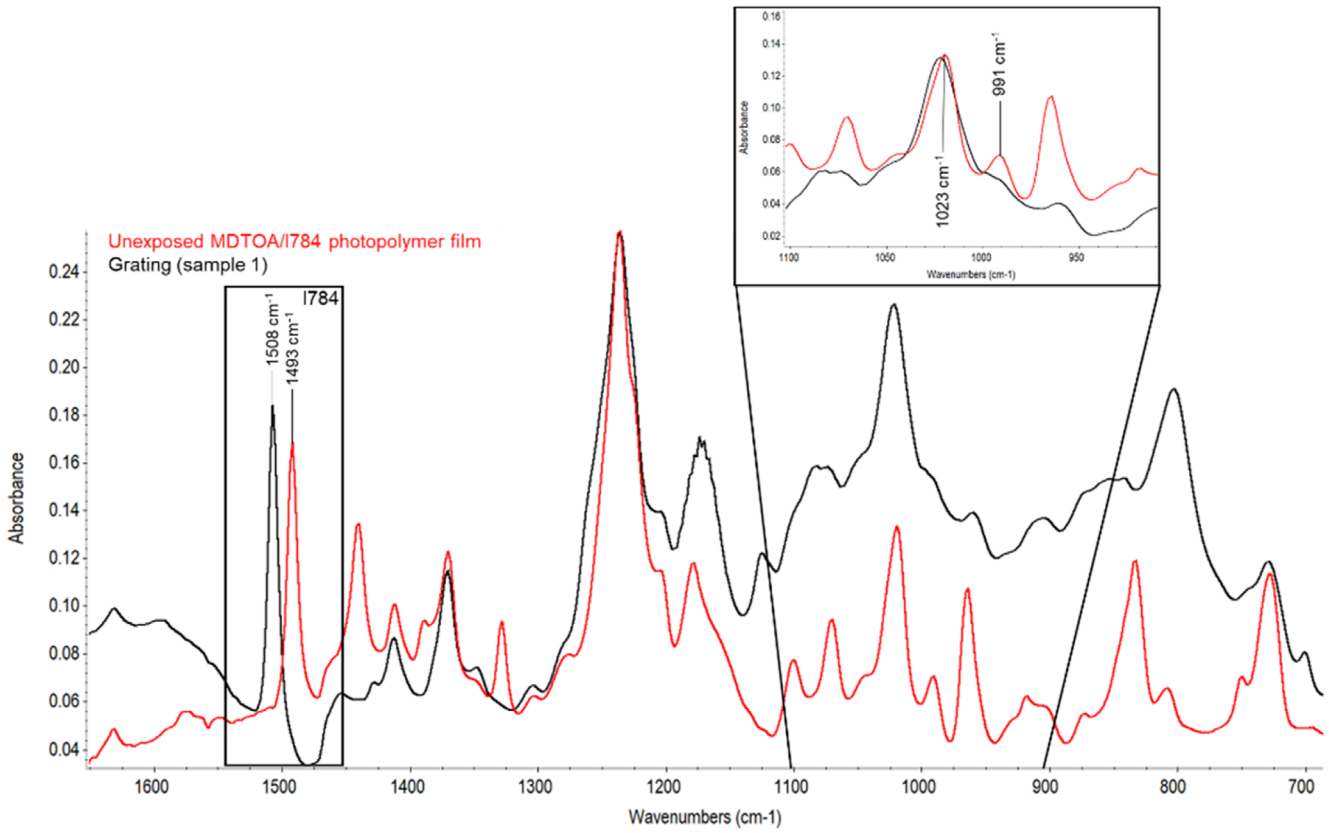

FIGURE 5 IR spectrum of the unexposed MDTOA/I784 photopolymer (red line) and of the bleached grating (sample 1, black line). The box shows the bands related to the I784 reaction. The inset highlights the band variation due to the polymerization reaction

disappearance of the monomer band at 991 cm^{-1}, which was also observed in Figure 4, and the shift of the band at 1022 cm^{-1}. As for I784, we observe the rise of the band at 1508 cm^{-1}, which is accompanied by the disappearance of the band at 1493 cm^{-1}, meaning that all the photoinitiator reacted. Though this analysis cannot be used to compute the monomer conversion, it clearly demonstrates the formation of the expected polymer structure.

Holographic writing tests of PETMP-containing photopolymers were also performed. Gratings at different MDTOA/thiol molar ratio were considered in order to determine the optimal thiol concentration. The diffraction efficiency curves are shown in Figure 6.

A clear positive effect of the presence of the thiol is the Δn increase. This improvement could be ascribed to both higher monomer conversion and thiol contribution to the polymer refractive index. The Δn also increases at increasing thiol concentration, with best results achieved when monomer and crosslinker are in stoichiometric ratio.[47] Under this condition, the Δn obtained is 0.0158, which notably corresponds to 86% of the formula limit. The shape of the diffraction efficiency curve is always nearly ideal and matches very well with the computed one. This indicates that the polymerization does not cause pattern distortions, as expected for thiol-ene systems, for which the formation of a crosslinked network is accompanied by low stress build up.[48–50] All gratings written with MDTOA/PETMP/I748 formulation are stable in time. Based on these results, only samples containing a stoichiometric amount of thiol with respect to MDTOA were further considered. It is important to note that step-growth polymerization reaction is intrinsically slower than a chain-growth polymerization. Indeed, comparing the monitoring curves (Figure 7) recorded during the writing step with and without thiol at same MDTOA concentration (sample 4 and 1 respectively), a significant difference is seen.

A writing dose of 1.2 J/cm^2 was required for writing the sample with the thiol, which is 2.5 times larger compared to the dose required for sample 1. On the other hand, inhibition time is greatly reduced (from 26 to 3.6 s) due to the presence of the thiol. This is not surprising since the thiol-ene polymerization is insensitive to oxygen.[51–53] Once the period of inhibition in sample 1 ends, it polymerizes faster than the thiol containing step growth polymerization of sample 4.

In order to understand how PETMP contributes to the final Δn, a sample with analogous formulation of

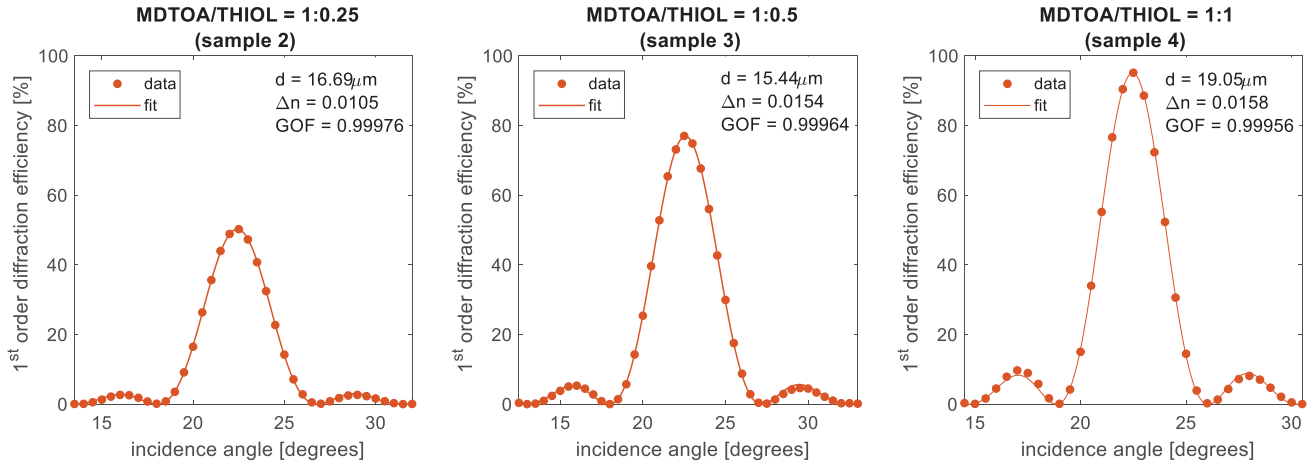

FIGURE 6 Diffraction efficiency curves of samples 2, 3, and 4 measured at 632.8 nm (p- polarization) as function of the incidence angle with relative fit with the Kogelnik equation

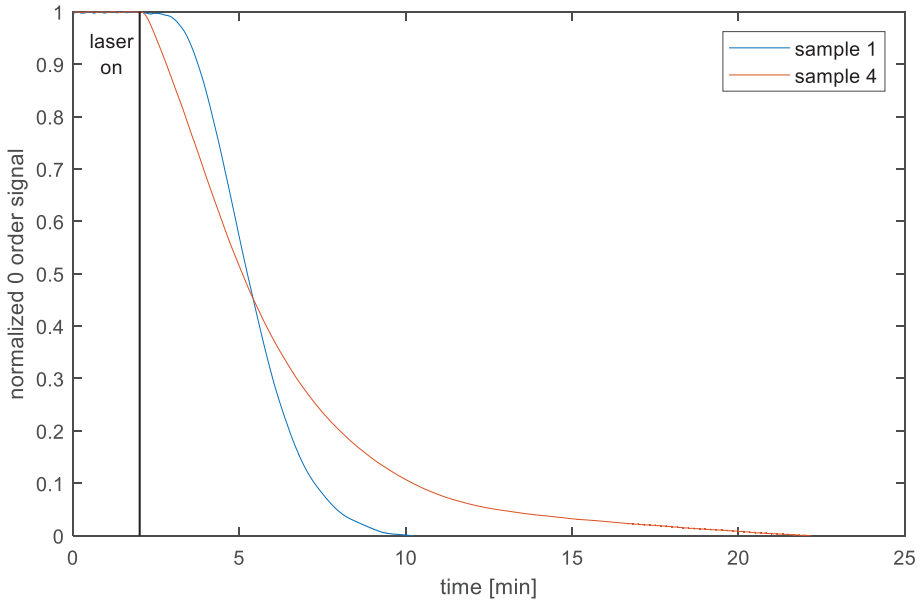

FIGURE 7 Normalized intensity of the probing laser at 850 nm during the holographic exposure of sample 1 and 4

sample 4 but without the MDTOA monomer was prepared (sample 10). It was demonstrated that it is possible to write a grating by thiol-thiol polymerization[54] of PETMP, and a Δn of 0.0114 was obtained in this case. Polymers with high content of S—S bonds in their backbone are indeed reported to show high refractive index.[55] However, the pattern resulted to be not completely stable over time, as a decrease of its diffraction efficiency of about 3% was observed after 1 week. The instability of the pattern could be due to the formation of short polymer chains that countermigrate after exposure. Therefore, the thiol gives a significant contribution to the refractive index modulation, but only by copolymerization with the MDTOA monomer, it guarantees the formation of a well-developed crosslinked network that remains stable in time. An evidence of the reaction between MDTOA and PETMP was obtained from IR analysis of the spectrum of the sample 4. Indeed, although a broad band seems to form in the 1700–1550 cm^{-1} region, probably due to some absorbed water (confirmed by the presence of a broad and weak band of the —OH stretching at 3500 cm^{-1}),[56] the disappearance of the C═C stretching band at 1632 cm^{-1} is clearly observed (Figure 8). This indicates that the two components copolymerize and that the thiols also react with the allyl bonds present in the polymer backbone to give a crosslinked network, as described before. Also in this case, we notice the variation of the 1508 and 1493 cm^{-1} bands due to the reaction of I784.

The dependence of Δn on the MDTOA concentration was studied in films containing a stoichiometric amount of thiol. The results are reported in Figure 9 together with

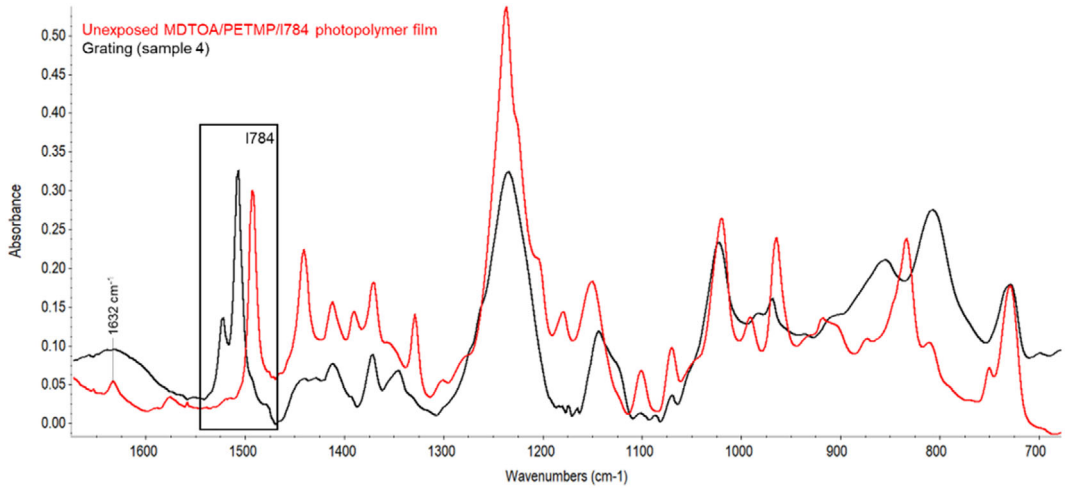

FIGURE 8 IR spectrum of the unexposed MDTOA/PETMP/I784 photopolymer (red line) and of the bleached grating (sample 4, black line). Band variation due to I784 reaction are highlighted in the box

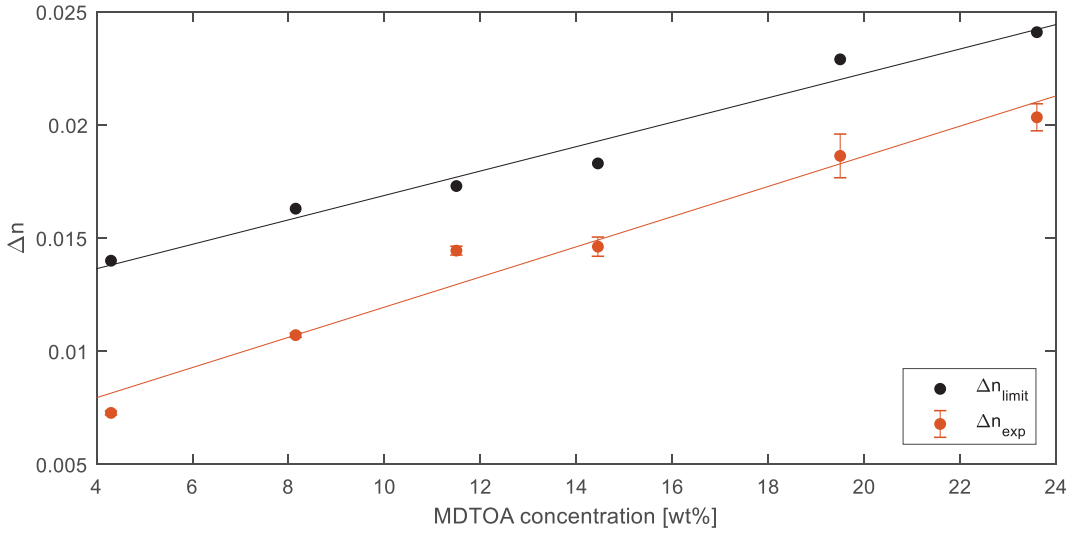

FIGURE 9 Experimental Δn of samples 4–9 (at 632.8 nm, unpolarized light) as function of the wt% concentration of MDTOA and corresponding $\mathbf{\Delta n_{limit}}$

the corresponding computed Δn_{limit} (as reported in Table 1).

We notice a linear increase of the measured values of Δn, which is consistent with the Δn_{limit} trend. It is important to underline that values of the order of 0.02 can be obtained, which are certainly large values especially considering the relatively small mismatch between the refractive index of binder and monomer.

2.3 | Thermal post process

Different studies reported in the literature show that the performances of CAB-based photopolymers can be improved by a thermal treatment.[37,38,57] This effect was studied on this new photopolymer formulation (details are reported in the experimental section). The thermal treatment was performed after the writing and bleaching of the film, and it was applied to films with and without the presence of the thiol crosslinker.

Without crosslinker (Figure 10(A)), a strong decrease of the diffraction efficiency is observed, which is correlated to a reduction of the refractive index modulation of a factor 6 (see Figure 3 for a comparison). This is probably caused by the diffusion of the polymer chains in the whole volume of the film to reach a condition of thermodynamic equilibrium. A change of the film thickness accompanies the process.

When the crosslinker is added to the formulation (Figure 10(B)), the effect of the thermal treatment is to

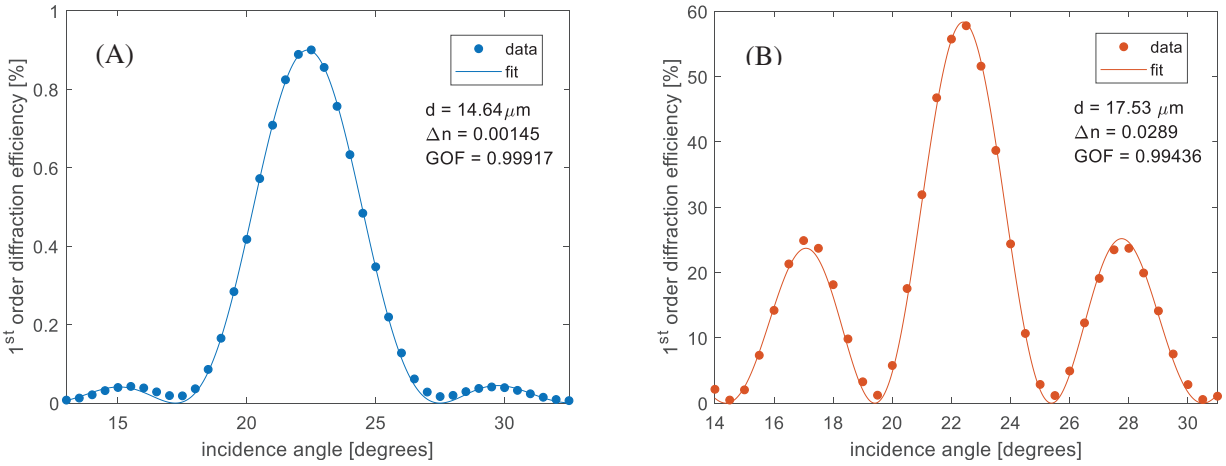

FIGURE 10 (A) Diffraction efficiency curve and Kogelnik fit of sample 1 measured at 632.8 nm (p- polarization) after the thermal treatment; (B) the same curve in the case of the presence of the crosslinker (sample 4)

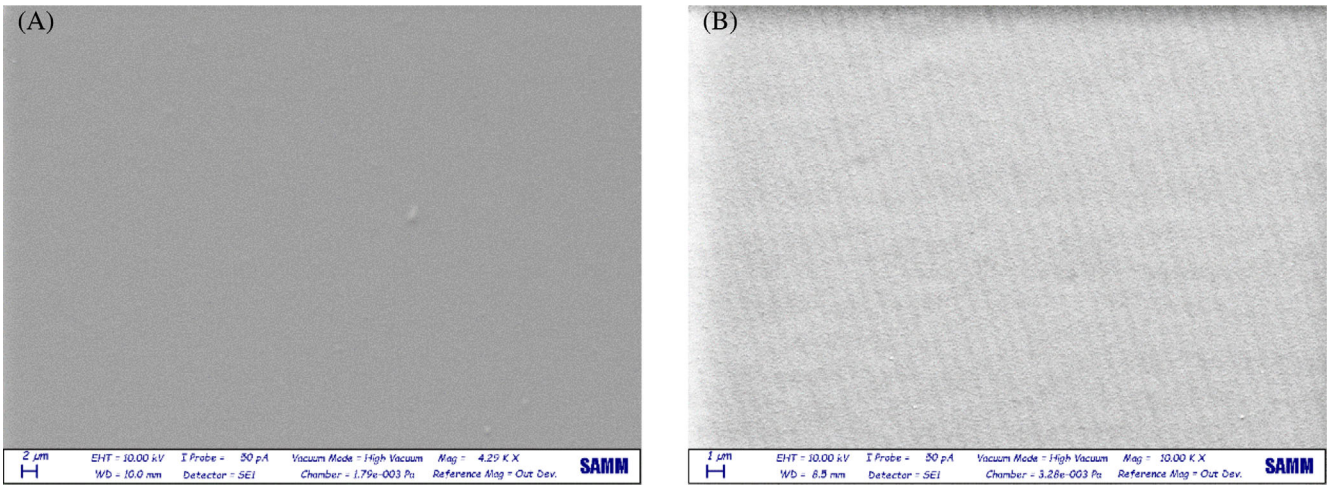

FIGURE 11 SEM images of sample 4 before (A) and after (B) the thermal treatment

promote an increase of the refractive index modulation and the curve appears overmodulated. Indeed, the Δn of sample 4 is almost doubled after the thermal treatment, as it increases from 0.0158 to 0.0289. The recorded enhancement of the refractive index modulation can be interpreted as a further diffusion of the writing chemistry. Indeed, during the writing of the grating, the forming polymer chains may grow also into dark areas.[58,59] Increasing the temperature and thus the mobility of the system, the crosslinked network is allowed to gather in bright areas. This process causes a marked separation of the writing chemistry from the binder and it is accompanied by a density increase. Both contributions account for an increase of the refractive index modulation. This process does not cause a deformation of the holographic pattern, as demonstrated by the recorded efficiency curve reported in Figure 10(B). Indeed, even if the sample is clearly overmodulated, the efficiency curve is still well fitted by the Kogelnik equation.

In spite of this indirect evidence, a morphological analysis of the surface was carried out to understand the modification induced by the thermal process. According to the SEM analysis, the surface of the sample appears completely smooth before the thermal treatment (Figure 11(A)), whereas a periodic modulation of the surface appears for the thermally treated sample (Figure 11(B)).

The period of the surface structure observed is of 0.83 μm, confirming the measured line density for the grating of 1204 lines/mm. The AFM analysis of the sample, reported in Figure 12, allowed to determine the peak-to-valley average height, which is 6 nm.

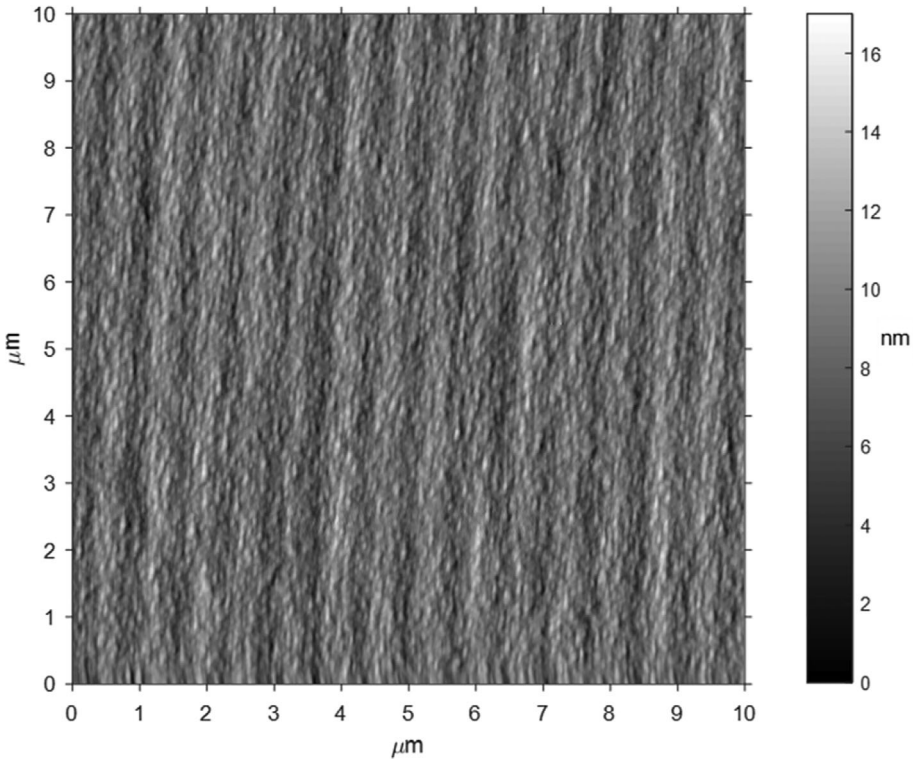

FIGURE 12 AFM analysis of sample 4 after the thermal treatment

Hence, the surface modulation is extremely limited. Indeed, the formation of the surface structure does not affect the VPHG diffraction properties, as apparent from the diffraction efficiency curve (Figure 10(B)).

To better understand the mechanism that leads to the Δn increase upon thermal treatment, the average refractive index (n_{ave}) of the bleached grating was measured before and after the thermal treatment. It decreased from 1.5163 to 1.5133. The refractive index of the background material, namely the film with all the components except the monomer and crosslinker, was also measured after the bleaching, and it resulted to be 1.4991. The Δn obtained before the thermal treatment corresponds to 0.0158 (Figure 6). This value is almost equal to the difference between the average refractive index of the grating and the bleached background material, showing that there is no much monomer left in the dark areas and the polymer chains have grown in the bright areas. Since the experiments have shown the modulation of the refractive index is actually affected by the thermal treatment, the diffusion of the polymer chains and oligomers likely supports this evidence. If we compare the Δn value obtained after the thermal treatment (0.0289) with the Δn_{limit} (0.0183), we notice that a value of 158% is achieved, and such value can be explained only with a change in the material density. In order to quantify it, we can describe the bright and dark regions of the photopolymer as an homogeneous material composed by a certain density N of Lorentz elements characterized by a polarizability α. The corresponding refractive index can be written as (Lorentz-Lorenz formula)[60,61]:

$$\frac{n^2-1}{n^2+2}=N\alpha \tag{1}$$

Knowing the average refractive index (n_{ave}) of the written film and the Δn, before and after the thermal treatment, we can calculate the refractive index of the bright (n_b) and dark (n_d) areas as follow:

$$n_b = n_{ave} + \Delta n \qquad n_d = n_{ave} - \Delta n \tag{2}$$

the values for the grating before ($n_b{}^G$, $n_d{}^G$) and after the thermal treatment ($n_b{}^{GT}$, $n_d{}^{GT}$) are reported in Table 2.

We assume that the polarizability does not change upon the thermal treatment; therefore, we make the ratio of Equation 1 for the bright and dark regions:

TABLE 2 Computed refractive index of the bright and dark fringes before and after thermal treatment

Refractive index	Value
n_b^G	1.5321
n_d^G	1.5005
n_b^{GT}	1.5422
n_d^{GT}	1.4844

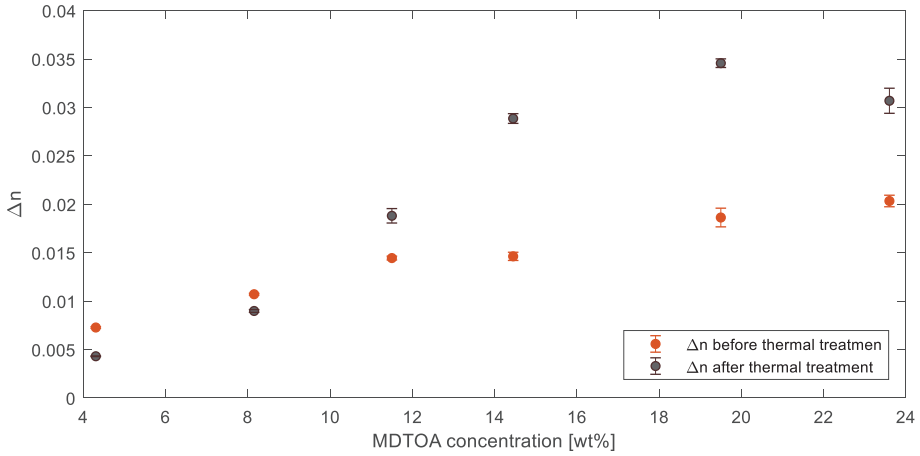

FIGURE 13 Δn of samples 4–9 (at 632.8 nm, unpolarized light) as function of the wt% concentration of MDTOA before and after the thermal treatment

$$\frac{n_b^{GT^2}-1}{n_b^{GT^2}+2}\times\frac{n_b^{G^2}+2}{n_b^{G^2}-1}=\frac{N_b^{GT}}{N_b^{G}} \qquad \frac{n_d^{GT^2}-1}{n_d^{GT^2}+2}\times\frac{n_d^{G^2}+2}{n_d^{G^2}-1}=\frac{N_d^{GT}}{N_d^{G}} \tag{3}$$

The density ratio is the parameter we are interested in and we obtain a change of density of +1.6% in written (bright) areas and −2.7% in unwritten (dark) areas. The fact that the density could either increase or decrease has been already reported in the literature.[62] This effect can be ascribed to the rearrangement of the polymer chains in bright areas: higher polymer chain packing leads to an increase of the material density; whereas, the density decrease might be due to the loss of volatile compounds from dark areas. To support this hypothesis, the change in weight of the written sample after the thermal treatment was measured. A mass loss of about 22% was observed, which can be ascribed to the sum of two contributions: (i) a uniform mass loss, which also determines the decrease of the film thickness after the thermal treatment, and (ii) a localized mass loss in unexposed areas of the grating which is responsible for the density decrease of these regions. The first contribution was determined to be as large as at least 10%, as measured for photopolymer films homogeneously illuminated and thermally treated analogously to the gratings, but it could be even larger in the case of the grating, for which a higher conversion of functional groups is expected.

Since the results of the thermal process were promising, its effect was studied as function of the MDTOA concentration (samples 4–9), for which different behaviors were observed (Figure 13).

At low MDTOA concentration, a small decrease of the refractive index modulation is obtained after the thermal treatment. In these cases, short polymer chains and oligomers are more likely to form. This prevents the formation of a stable network and allows the oligomers to migrate during the thermal treatment with a redistribution also in the dark areas. Above a certain monomer concentration, that is 11.5 wt% for this photopolymer system (sample 7), this phenomenon has a low probability to occur, leading to a Δn increase. The effect of the thermal treatment becomes more relevant at higher monomer concentration and a remarkably high refractive index modulation of 0.0346 is achieved at 19.5 wt% (sample 8). Such value is among the largest reported in the literature for photopolymeric systems.[24,25,31,63] Increasing even more the concentration up to 23.6 wt% (sample 9) does not induce a Δn increase as high as expected. In that case, a saturation of polymer concentration in the high index regions could cause end chains to remain in dark areas, mitigating the index modulation.

3 | CONCLUSIONS

We developed a new photopolymer formulation based on the CAS monomer 7-methylene-1,5-dithiacyclooctan-3-yl acetate which allows for a very high refractive index modulation that is increased from 35% to 86% of the formula limit by addition of a thiol to the formulation. The selected tetrafunctional thiol also enables the formation of a crosslinked network, which allows for a further remarkable increase of the Δn by a thermal treatment. For the effectiveness of this post process, a lower and upper limit of monomer concentration exists. The highest Δn is obtained at 19.5 wt% of MDTOA, reaching a value of 0.0346, which is one of the largest value reported in the literature so far. The huge increase of the refractive index modulation can be explained as a diverse density variation in the written and unwritten areas, as confirmed by combining SEM and AFM analysis and refractive index measurements.

4 | EXPERIMENTAL SECTION

Materials: cellulose acetate butyrate (CAB-531-1) was provided by Eastman, pentaerythritol tetrakis(3-mercaptopropionate) (PETMP) was purchased from TCI, bis (2,6-difluoro-3-[1-hydropyrrol-1-yl]phenyl)titanocene (also known as Irgacure® 784, I784) was purchased from Gelest, tris(2-ethylhexyl) O-acetylcitrate (Citrofol® AHII) was purchased from Jungbunzlauer, butyl acetate was purchased from Sigma–Aldrich. All chemical reagents were used as received. The cyclic allylic sulfide monomer 7-methylene-1,5-dithiacyclooctan-3-yl acetate (MDTOA) was synthesized following the procedure detailed in Ref. [33]. The synthetic route, shown in Scheme 3, consists first in a one-pot two-step formation of the 3-mercapto-2-(mercaptomethyl)-1-propene (2) starting from the 3-chloro-2-(chloromethyl)-1-propene, which reacts with an excess of o-ethylxanthic acid potassium salt in absolute ethanol under inert conditions to give the bis-xantane (1), followed by the liberation of 3-mercapto-2-(mercaptomethyl)-1-propene (2). Worth noting, the last step has to be carefully performed, by adding dropwise the bis-xantane into ethylenediamine so as not to increase the temperature above 30°C. The workup involves an acidic treatment in H_2SO_4, extraction and bulb-to bulb distillation of the organic layer.

The obtained 3-mercapto-2-(mercaptomethyl)-1-propene (2) is then coupled with stoichiometric 1,3-dibromo-2-propanol in ethanol, under reflux in inert ambient. The raw product is purified by flash chromatography giving 7-methylene-1,5-dithiacyclooctan-3-ol (3) as a white powder. As the last step, acetyl chloride in ether is added dropwise to a cooled solution of 7-methylene-1,-5-dithiacyclooctan-3-ol and triethylamine in dry ether and refluxed for 1 h. The raw product is purified by extraction and flash chromatography to give the desired 7-methylene-1,5-dithiacyclooctan-3-yl acetate (MDTOA) as a clear solid.

^{1}H NMR ($CDCl_3$), δ (ppm): 2.03 (s, 3H, —CH_3), 3.04 (apparent d, 4H, J = 5.2 Hz, —SCH_2—CHO—), 3.24 (s, 4H, allylic —CH_2—), 5.01 (apparent pent, 1H, J = 5.3 Hz), 5.24 (s, 2H, dCH_2).

Film preparation: CAB, MDTOA, PETMP and the plasticizer were dissolved in butyl acetate using the concentrations reported in Table 1. The photoinitiator I784 was then added to the formulation. The solution was stirred for at least 4 h and sonicated to remove air bubbles before deposition. The films were produced by bar-coating (RK K Control Coater) on glass substrates obtaining thicknesses in the range of 15–20 μm. All the operations were carried out in a dark room to avoid unwanted light-induced polymerization. The films were stored overnight before use to let the solvent evaporate completely.

Refractive index measurements: the refractive index of the photopolymer was measured with an Abbe refractometer using white light and at room temperature depositing the solution directly on the refracting prism.

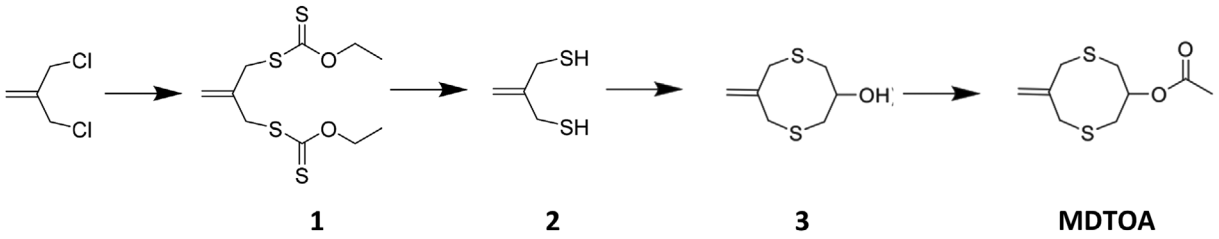

SCHEME 3 Synthetic route to yield MDTOA.[33]

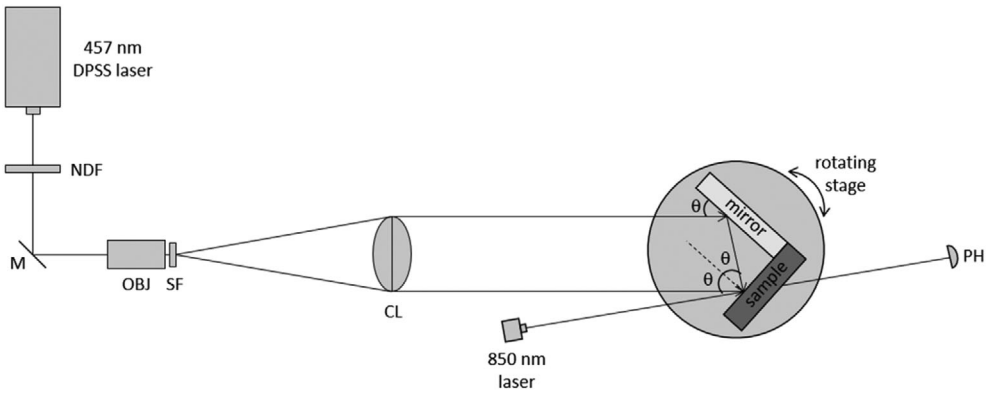

FIGURE 14 Lloyd mirror setup for the writing of transmission gratings. CL, collimating lens; M, mirror; NDF, neutral density filter; OBJ, microscope objective; PH, photodiode; SF, spatial filter

Measurements were performed after complete solvent evaporation.

Holographic recording: transmission gratings were recorded using a Lloyd mirror setup, schematized in Figure 14, set to obtain a line density of 1200 lines/mm (corresponding to a θ angle of 15.9° at the laser wavelength used). Such value was chosen in order to be in Bragg regime[64] during the characterization phase and thus to be able to apply the Kogelnik equation[65] to fit the diffraction efficiency curves. During the writing of the hologram, the photopolymer film was coupled with an OG570 filter with an index matching oil to minimize the back reflections and oxygen inhibition.

A 457 nm DPSS laser (Cobolt Twist™ 200) with intensity of 1 mW/cm^2 was used for the writing, while a 850 nm diode laser incident to the sample at Bragg's angle (30.6°) was used to probe the hologram formation, monitoring in real time the signal of the zero order. The exposure time was varied for each sample in order to reach the maximum conversion (plateau of the 850 nm laser signal). After the writing of the grating, the samples were completely bleached by exposure to a white LED (for 10 min at a power density of 20 mW/cm^2), ensuring good transparency of the film in all the visible range. Gratings with dimension of 20 × 14 mm were recorded. The diffraction efficiency of the VPHG was measured with a He-Ne 632.8 nm laser (Thorlabs, HNL020LB) in both s- and p- polarizations as function of the incident angle. The experimental curves, corrected for reflection losses were fitted with the Kogelnik equation, in which the film thickness (d) and the refractive index modulation (Δn) were the free parameters of the fit. The line density of each grating was measured independently.

FTIR analysis: spectra were collected with a JASCO FT/IR-4600 spectrophotometer with resolution of 2 cm^{-1} and 64 scans. For the recording of the spectra of the photopolymer formulations and of the polymeric matrix, thin films were deposited by spin coating (POLOS 200, revolution speed of 500 rpm) on ZnSe substrates. Spectra of the gratings were obtained detaching the films from the glass substrate and placing them directly in the spectrophotometer.

Thermal treatment: samples were placed in an oven (Falc STZ18) at 120°C for 2.5 h after the writing of the VPHG. The duration and temperature of the treatment were optimized for this photopolymer system. The mass loss of thermally treated samples was determined by weighing them before and after the thermal treatment. The samples considered were gratings and bleached films deposited on glass substrates. In the case of gratings, the samples were cut in order to consider only the written area of the film.

SEM and AFM analysis: SEM analysis of the grating was performed with a ZEISS EVO 50VP made in high vacuum mode at 10 kV EHT and with a probe current of 50 pA. The surface of the films was golden coated to ensure the correct conductivity of the sample during the measurements. AFM surface morphology was recorded with a NT-MDT Solver Pro in contact mode using a CSG01 tip.

ACKNOWLEDGEMENTS

This work was partially supported by OPTICON project (funded by the European Union's Horizon 2020 research and innovation programme under grant agreement No 730890) and by HYPERMAT project (Fondazione Cariplo, Regione Lombardia, "Materiali Avanzati" 2018).

CONFLICT OF INTEREST

The authors declare no potential conflict of interest.

ORCID

Paola Galli https://orcid.org/0000-0002-4812-8471
Chiara Bertarelli https://orcid.org/0000-0002-4577-0741
Andrea Bianco https://orcid.org/0000-0002-7691-404X

REFERENCES

[1] J. Jialing, C. Lin, W. Xiqiao, G. Jinxin, W. Dayong, Z. Xinping, *Opto-Electron. Eng.* **2019**, *46*, 180552.
[2] T. Lloret, V. Navarro-Fuster, M. G. Ramírez, M. Ortuño, C. Neipp, A. Beléndez, I. Pascual, *Polymers* **2018**, *10*, 302.
[3] A. Khan, G. D. Stucky, C. J. Hawker, *Adv. Mater.* **2008**, *20*, 3937.
[4] A. Khan, A. E. Daugaard, A. Bayles, S. Koga, Y. Miki, K. Sato, J. Enda, S. Hvilsted, G. D. Stucky, C. J. Hawker, *Chem. Commun.* **2009**, *4*, 425.
[5] R. Fernández, S. Bleda, S. Gallego, C. Neipp, A. Márquez, Y. Tomita, I. Pascual, A. Beléndez, *Opt. Express* **2019**, *27*, 827.
[6] R. Malallah, H. Li, P. D. Kelly, J. J. Healy, T. J. Sheridan, *Polymer* **2017**, *9*, 9.
[7] F.-K. Bruder, R. Hagen, T. Rölle, M.-S. Weiser, T. Fäcke, *Angew. Chemie Int. Ed.* **2011**, *50*, 4552.
[8] Y. Tomita, E. Hata, K. Momose, S. Takayama, X. Liu, K. Chikama, J. Klepp, C. Pruner, M. Fally, *J. Mod. Opt.* **2016**, *63*, S1.
[9] J. T. Sheridan, R. K. Kostuk, A. G. Fimia, Y. Wang, W. Lu, H. Zhong, Y. Tomita, C. Neipp, J. Francés, S. Gallego, I. Pascual, V. Marinova, S. H. Lin, K. Y. Hsu, F. K. Bruder, S. Hansen, C. Manecke, R. Meisenheimer, C. Rewitz, T. Rölle, S. Odinokov, O. Matoba, M. Kumar, X. Quan, Y. Awatsuji, P. W. Wachulak, A. Gorelaya, A. Sevryugin, E. Shalymov, V. Venediktov, R. Chmelik, M. A. Ferrara, G. Coppola, A. Marquez, A. Belendez, W. Yang, R. Yuste, A. Bianco, A. Zanutta, C. Falldorf, J. Healy, X. Fan, B. Hennelly, I. Zhurminsky, M. Schnieper, R. Ferrini, S. Fricke, G. Situ, H. Wang, A. Abdurashitov, V. V. Tuchin, N. Petrov, T. Nomura, D. Morim, K. Saravanamuttu, *J. Opt.* **2020**, *22*, 123002.
[10] F.-K. Bruder, T. Fäcke, T. Rölle, *Polymers* **2017**, *9*, 472.
[11] F.-K. Bruder, J. Frank, S. Hansen, R. Künzel, C. Manecke, R. Meisenheimer, J. Mills, L. Pitzer, T. Rölle, B. Wewer, in *Proc. SPIE*, **2020**, *11367*.

[12] F.-K. Bruder, T. Fäcke, F. Grote, R. Hagen, D. Hönel, E. Koch, C. Rewitz, G. Walze, B. Wewer, in *Proc. SPIE* **2017**, *10233*.
[13] B. J. Chang, C. D. Leonard, *Appl. Opt.* **1979**, *18*, 2407.
[14] X. Liang-wen, L. Shihong, P. Bi-xian, *Appl. Opt.* **1998**, *37*, 3678.
[15] H. I. Bjelkhagen, *Silver-Halide Recording Materials for Holography and their Processing*, Springer-Verlag, Berlin Heidelberg **1993**.
[16] W. S. Colburn, K. A. Haines, *Appl. Opt.* **1971**, *10*, 1636.
[17] G. Zhao, P. Mouroulis, *J. Mod. Opt.* **1994**, *41*, 1929.
[18] D. Graham-Rowe, *Nat. Photonics* **2007**, *1*, 197.
[19] M. Haw, *Nature* **2003**, *422*, 556.
[20] L. Dhar, *MRS Bull.* **2006**, *31*, 324.
[21] K. Mitsube, Y. Nishimura, K. Nagaya, S. Takayama, Y. Tomita, *Opt. Mater. Express* **2014**, *4*, 982.
[22] E. Hata, Y. Tomita, *Opt. Lett.* **2010**, *35*, 396.
[23] Y. Tomita, H. Urano, T. Fukamizu, Y. Kametani, N. Nishimura, K. Odoi, *Opt. Lett.* **2016**, *41*, 1281.
[24] A. Narita, J. Oshima, Y. Iso, S. Hasegawa, Y. Tomita, *Opt. Mater. Express* **2021**, *11*, 614.
[25] Y. Tomita, T. Aoi, S. Hasegawa, F. Xia, Y. Wang, J. Oshima, *Opt. Express* **2020**, *28*, 28366.
[26] B. A. Kowalski, A. C. Urness, M.-E. Baylor, M. C. Cole, W. L. Wilson, R. R. McLeod, *Opt. Mater. Express* **2014**, *4*, 1668.
[27] B. A. Kowalski, R. R. McLeod, *J. Polym. Sci. Part B Polym. Phys.* **2016**, *54*, 1021.
[28] M. D. Alim, D. J. Glugla, S. Mavila, C. Wang, P. D. Nystrom, A. C. Sullivan, R. R. McLeod, C. N. Bowman, *ACS Appl. Mater. Interfaces* **2018**, *10*, 1217.
[29] C. R. Morgan, F. Magnotta, A. D. Ketley, *J. Polym. Sci. Polym. Chem. Ed.* **1977**, *15*, 627.
[30] C. E. Hoyle, T. Y. Lee, T. Roper, *J. Polym. Sci. Part A Polym. Chem.* **2004**, *42*, 5301.
[31] Y. Hu, B. A. Kowalski, S. Mavila, M. Podgórski, J. Sinha, A. C. Sullivan, R. R. McLeod, C. N. Bowman, *ACS Appl. Mater. Interfaces* **2020**, *12*, 44103.
[32] R. A. Evans, E. Rizzardo, *Macromolecules* **1996**, *29*, 6983.
[33] R. A. Evans, E. Rizzardo, *Macromolecules* **2000**, *33*, 6722.
[34] R. A. Evans, E. Rizzardo, *J. Polym. Sci. Part A Polym. Chem.* **2001**, *39*, 202.
[35] D. A. Waldman, H.-Y. S. Li, M. G. Horner, *J. Imaging Sci. Technol.* **1997**, *41*, 497.
[36] K. Choi, J. W. M. Chon, M. Gu, N. Malic, R. A. Evans, *Adv. Funct. Mater.* **2009**, *19*, 3560.
[37] W. K. Smothers, B. M. Monroe, A. M. Weber, D. E. Keys, *Proc. SPIE* **1990**, *1212*, 20.
[38] W. J. J. Gambogi, A. M. Weber, T. J. Trout, *Proc. SPIE* **1994**, *2043*, 2.
[39] H. Yoon, H. Yoon, S.-H. Paek, J. H. Kim, D. H. Choi, *Opt. Mater.* **2005**, *27*, 1190.
[40] C. E. Hoyle, C. N. Bowman, *Angew. Chemie Int. Ed.* **2010**, *49*, 1540.
[41] S. H. Lin, Y.-N. Hsiao, K. Y. Hsu, *J. Opt. A Pure Appl. Opt.* **2009**, *11*, 24012.
[42] D. Sabol, M. R. Gleeson, S. Liu, J. T. Sheridan, *J. Appl. Phys.* **2010**, *107*, 53113.
[43] P. Galli, R. A. Evans, C. Bertarelli, A. Bianco, *Proc. SPIE* **2020**, *1136711*, 1.
[44] R. A. Evans, G. Moad, E. Rizzardo, S. H. Thang, *Macromolecules* **1994**, *27*, 7935.
[45] M. T. Devlin, V. F. Kalasinsky, I. W. Levin, *J. Mol. Struct.* **1989**, *213*, 35.
[46] G. Socrates, *Infrared and Raman Characteristic Group Frequencies: Tables and Charts*, Wiley, Chichester **2004**.
[47] E. Hata, Y. Tomita, *Opt. Mater. Express* **2011**, *1*, 1113.
[48] B.-S. Chiou, R. J. English, S. A. Khan, *Macromolecules* **1996**, *29*, 5368.
[49] B.-S. Chiou, S. A. Khan, *Macromolecules* **1997**, *30*, 7322.
[50] B.-S. Chiou, S. Khan, *Photopolymerization Fundamentals and Applications*, American Chemical Society, Washington, DC **1997**.
[51] M. R. Zonca, B. Falk, J. V. Crivello, *J. Macromol. Sci. Part A* **2004**, *41*, 741.
[52] C. Nason, T. Roper, C. Hoyle, J. A. Pojman, *Macromolecules* **2005**, *38*, 5506.
[53] T. M. Roper, T. Kwee, T. Y. Lee, C. A. Guymon, C. E. Hoyle, *Polymer* **2004**, *45*, 2921.
[54] N. Feillée, M. De Fina, A. Ponche, C. Vaulot, S. Rigolet, L. Jacomine, H. Majjad, C. Ley, A. Chemtob, *J. Polym. Sci. Part A Polym. Chem.* **2017**, *55*, 117.
[55] J. Liu, M. Ueda, *J. Mater. Chem.* **2009**, *19*, 8907.
[56] B. L. Mojet, S. D. Ebbesen, L. Lefferts, *Chem. Soc. Rev.* **2010**, *39*, 4643.
[57] A. M. Weber, W. K. Smothers, T. J. Trout, D. J. Mickish, *Proc. SPIE* **1990**, *1212*, 30.
[58] J. T. Sheridan, J. R. Lawrence, *J. Opt. Soc. Am. A* **2000**, *17*, 1108.
[59] M. R. Gleeson, J. V. Kelly, D. Sabol, C. E. Close, S. Liu, J. T. Sheridan, *J. Appl. Phys.* **2007**, *102*, 23108.
[60] L. Lorenz, *Ann. Phys.* **1880**, *247*, 70.
[61] H. A. Lorentz, *Ann. Phys.* **1880**, *245*, 641.
[62] S.-D. Wu, E. N. Glytsis, *J. Opt. Soc. Am. B* **2004**, *21*, 1722.
[63] F.-K. Bruder, J. Frank, S. Hansen, A. Lorenz, C. Manecke, R. Meisenheimer, J. Mills, L. Pitzer, I. Pochorovski, in *Proc. SPIE* **2021**, *11710*, 1.
[64] M. G. Moharam, L. Young, *Appl. Opt.* **1978**, *17*, 1757.
[65] H. Kogelnik, *Landmark Pap. Photorefractive Nonlinear Opt*, World Scientific, **1995**, p. 133.

How to cite this article: Galli P, Evans RA, Bertarelli C, Bianco A. Cyclic allylic sulfide based photopolymer for holographic recording showing high refractive index modulation. *J Polym Sci*. 2021;59:1399–1413. https://doi.org/10.1002/pol.20210192